

AD \_\_\_\_\_

Award Number: DAMD17-98-1-8211

TITLE: Analysis of Interval Changes on Mammograms for Computer  
Aided Diagnosis

PRINCIPAL INVESTIGATOR: Lubomir Hadjiiski, Ph.D.

CONTRACTING ORGANIZATION: University of Michigan  
Ann Arbor, Michigan 48109-1274

REPORT DATE: May 2001

TYPE OF REPORT: Annual Summary

PREPARED FOR: U.S. Army Medical Research and Materiel Command  
Fort Detrick, Maryland 21702-5012

DISTRIBUTION STATEMENT: Approved for Public Release;  
Distribution Unlimited

The views, opinions and/or findings contained in this report are those of the author(s) and should not be construed as an official Department of the Army position, policy or decision unless so designated by other documentation.

20010723 131

**REPORT DOCUMENTATION PAGE**Form Approved  
OMB No. 074-0188

Public reporting burden for this collection of information is estimated to average 1 hour per response, including the time for reviewing instructions, searching existing data sources, gathering and maintaining the data needed, and completing and reviewing this collection of information. Send comments regarding this burden estimate or any other aspect of this collection of information, including suggestions for reducing this burden to Washington Headquarters Services, Directorate for Information Operations and Reports, 1215 Jefferson Davis Highway, Suite 1204, Arlington, VA 22202-4302, and to the Office of Management and Budget, Paperwork Reduction Project (0704-0188), Washington, DC 20503

**1. AGENCY USE ONLY (Leave blank)****2. REPORT DATE**  
May 2001**3. REPORT TYPE AND DATES COVERED**

Annual Summary (6 Apr 00 - 5 Apr 01)

**4. TITLE AND SUBTITLE**

Analysis of Interval Changes on Mammograms for Computer Aided Diagnosis

**5. FUNDING NUMBERS**

DAMD17-98-1-8211

**6. AUTHOR(S)**

Lubomir Hadjiiski, Ph.D.

**7. PERFORMING ORGANIZATION NAME(S) AND ADDRESS(ES)**University of Michigan  
Ann Arbor, Michigan 48109-1274**E-MAIL:**

lhadjisk@umich.edu

**8. PERFORMING ORGANIZATION REPORT NUMBER****9. SPONSORING / MONITORING AGENCY NAME(S) AND ADDRESS(ES)**U.S. Army Medical Research and Materiel Command  
Fort Detrick, Maryland 21702-5012**10. SPONSORING / MONITORING AGENCY REPORT NUMBER****11. SUPPLEMENTARY NOTES****12a. DISTRIBUTION / AVAILABILITY STATEMENT**

Approved for public release; distribution unlimited

**12b. DISTRIBUTION CODE****13. ABSTRACT (Maximum 200 Words)**

A multistage regional registration technique (MRRT) was developed for identifying masses on temporal pairs of mammograms. It was investigated the use of the density-weighted contrast enhancement (DWCE) technique to improve the localization of the corresponding mass on the prior mammogram. 179 temporal pairs of mammograms containing biopsy-proven masses were used for evaluation. 84% of the estimated lesion locations resulted in an area overlap of at least 50% with the true lesion locations. The average distance between the estimated and the true centroid of the lesions on the prior mammogram was  $4.8 \pm 6.9$  mm. The registration accuracy was improved in comparison with the registration without DWCE.

Regions of interest containing the corresponding masses were identified on the current and prior mammograms of the temporal pair. The masses were automatically segmented using a K-means clustering algorithm and active contour model. Texture, spiculation and morphological features were extracted from each mass. An additional difference features were obtained by subtracting the features of the prior mass from those of the current mass. The feature space for each temporal pair consisted of the texture, spiculation and morphological features from both the prior and the current mammograms and the difference features.

MRRT can be useful for identification of corresponding lesions on temporal pairs of mammograms. The obtained features will be used for classification of malignant and benign temporal masses as well as detection of temporal change.

**14. SUBJECT TERMS**

Breast Cancer, Computer-aided diagnosis, Screening, Classification, Image Analysis

**15. NUMBER OF PAGES**

27

**16. PRICE CODE****17. SECURITY CLASSIFICATION OF REPORT**

Unclassified

**18. SECURITY CLASSIFICATION OF THIS PAGE**

Unclassified

**19. SECURITY CLASSIFICATION OF ABSTRACT**

Unclassified

**20. LIMITATION OF ABSTRACT**

Unlimited



**(4) Table of Contents**

(1) Front Cover ..... 1

(2) Standard Form (SF) 298, REPORT DOCUMENTATION PAGE ..... 2

(3) FOREWORD ..... 3

(4) Table of Contents ..... 4

(5) Introduction ..... 5

(6) Body ..... 6

    (A) Database collection and extraction of regions of interest ..... 6

    (B) Further developments of methods for establishing corresponding locations in  
        current and previous mammograms ..... 6

    (C) Identify technique to be used in the first stage of segmentation ..... 7

    (D) Develop deformable object boundary models for boundary refinement and second  
        stage segmentation ..... 7

    (E) Obtaining hand drawn mass boundaries from radiologists and evaluation of  
        segmentation accuracy ..... 8

    (F) Develop methods for extracting morphological and texture features from masses  
        segmented from ROIs extracted from current and prior mammograms ..... 9

    (G) Analyze techniques for characterizing differences in these features ..... 10

(7) Conclusion ..... 11

(8) References ..... 11

(9) Appendix ..... 14

## **(5) Introduction**

Treatment of breast cancer at an early stage can significantly improve the survival rate of patients. Mammography is currently the most sensitive method for detecting early breast cancer [1, 2], and it is also the most practical for screening. Although general rules for the differentiation between malignant and benign lesions exist, in clinical practice, only 15-30% of cases referred for surgical biopsy are actually malignant. A number of research groups are in the process of developing computer-aided diagnosis (CAD) methods which can provide a second opinion to the radiologist for the detection and classification of breast abnormalities.

Radiologists routinely use several mammograms of different views of a patient with those obtained in previous years for identifying interval changes, detecting potential abnormalities, and in evaluating breast lesions. It is widely accepted that interval changes in mammographic features are very useful for both detection and classification of breast abnormalities. Some existing CAD techniques use information from multiple views of the same breast. Others use previous mammograms for detection. However none incorporates information about the temporal mammographic changes in the breast tissue for classification.

The goal of this project is to evaluate the usefulness of using interval changes to distinguish between normal structures, benign masses, and malignant masses in CAD. The purpose of this study is summarized as follows: 1. Characterize temporal changes in terms of the mammographic features of normal breast structures, as well as benign and malignant masses. 2. Use this information to develop methods for CAD. We hypothesize that the use of temporal changes in mammographic features between current and previous mammograms of the patient will improve the success of CAD technique for classification of masses. It is therefore expected that the use of such temporal information will improve the positive predictive value of mammography by reducing benign biopsies, and hence reduce both cost and patient morbidity.

To accomplish this goal we will first develop and evaluate reliable techniques for the temporal regional registration of mammograms of the same patient. The temporal mammogram registration technique we have developed is a novel approach in which the computer emulates the search method used by many radiologists for finding corresponding structures on mammograms. The method aims at registering a small region containing a suspected mass on the most recent mammogram of the patient with one on a mammogram obtained from a previous year. Our regional registration technique involves three steps: (1) identification of a suspicious structure on the most recent mammogram, (2) initial estimation of the location on a previous mammogram of the region corresponding to the suspicious structure and the definition of a search region which encloses the object of interest on the previous mammogram, and (3) accurate identification of the location of the matched object within the search region. The characteristic features of the two matched lesions then will be automatically extracted and interval changes estimated. This interval change information will be incorporated in an integrated CAD system.

## **(6) Body**

In the third year (4/6/00-4/5/01) of this grant, we have performed the following studies:

### **(A) Database collection and extraction of regions of interest (Task 1)**

We continued collecting the data set for this study from the files of patients who had undergone biopsy at the University of Michigan. The mammograms are scanned and the images are saved in our storage device using automated graphic user interface developed in our laboratory. Additionally the film information is recorded in a Microsoft Access database. Temporal pairs of images were obtained. The current mammogram of each temporal pair exhibited a biopsy-proven mass. We scan both cranio-caudal and mediolateral-oblique views. The mammograms were digitized with a LUMISCAN 85 laser scanner at a pixel resolution of 0.05 mm x 0.05 mm and with 12-bit resolution.

While the regional registration technique can be used for determining a corresponding structure or region for any structure (both normal tissues and masses) in the breast, in this study we are analyzing its accuracy on biopsy-proven masses alone. The location of the mass on the current mammogram identified by an MQSA-approved radiologist experienced in breast imaging using an interactive image analysis tool on a UNIX workstation. To provide the ground truth for evaluation of the computerized method, the radiologist manually identifies the corresponding region on the previous mammogram. Bounding boxes enclosing the mass on the current mammogram and the corresponding object on the previous mammogram are also provided by the radiologist for each case. Each mass as well as the corresponding structure on the previous mammogram are rated for its visibility on a scale of 1 to 10, where the rating of 1 corresponded to the most visible category. The size of the mass on the current mammogram as well as the size of the corresponding structure on the previous mammogram are also measured by the radiologist. The parenchymal density is rated based on the BI-RADS lexicon.

### **(B) Further developments of methods for establishing corresponding locations in current and previous mammograms (Task 3)**

We will continue to improve our regional registration technique [3-6]. In the first step, an automated method will be developed to detect the nipple location in the breast image. The method will be based on both the change of tangential direction and the change in the tissue density along the breast border. In the third step we have investigated the use of the density-weighted contrast enhancement (DWCE) technique to improve the localization of the corresponding mass on the prior mammogram. After the location of the fan-shaped region was refined by affine transformation and simplex optimization [5], [6], the DWCE technique was used to segment dense structures within the search region. A search for the best match between the lesion template from the current mammogram and a structure on the prior mammogram was performed within the DWCE segmented densities.

The regional registration technique has been evaluated with a data set of 179 temporal pairs of mammograms.

In this study 84% of the estimated lesion locations resulted in an area overlap of at least 50% with the true lesion locations. The average distance between the estimated and the true centroids of the lesions on the prior mammogram was  $4.8 \pm 6.9$  mm with a maximum of 46.6 mm. For the 84% of

the temporal pairs with 50% overlap, the average distance between the estimated and the true centroids of the lesions on the prior mammogram was  $2.5 \pm 2.5$  mm with a maximum of 10.2 mm.

The preliminary results of this study are promising. The DWCE segmentation improved the accuracy of matching by directing the search to the dense structures and thus reducing the chance of mismatch. The average Euclidean distance between the computer estimate of the corresponding structure and the radiologist-identified location and their standard deviation were both reduced when compared to multistage registration without DWCE segmentation. We presented the preliminary results on this improved method at the World Congress on Medical Physics and Biomedical Engineering, Chicago, July 23 - 28, 2000 [7].

### **(C) Identify technique to be used in the first stage of segmentation (Task 7)**

The ROIs were first processed with a background correction algorithm which aims at reducing the nonuniform background caused by the overlapping breast structures and the location of the lesion on the mammogram. The nonuniform background is not related to mass malignancy, but may affect the segmentation and feature extraction results used in our computerized analysis.

The mass segmentation method employed in this study started with the initial detection of a mass shape within an ROI using a pixel-by-pixel K-means clustering algorithm, which was discussed in detail in the literature [8]. The parameters of the segmentation algorithm were chosen so that the segmented region was slightly smaller than the actual size of the mass. This choice prevented most of the masses from merging into neighboring objects. After clustering, one to several objects would be segmented in the ROI. If more than one object was segmented, the largest connected object was selected. The selected object was then filled, grown in a local neighborhood, and eroded and dilated with morphological operators. In the resulting binary image, a nonzero value indicated an object pixel, and zero value indicated a background pixel.

Generally we were satisfied by the results obtained by the K-means clustering algorithm for the initial mass segmentation. The clustering resulted in reasonable mass shapes for almost all of the masses. We concentrated our efforts towards development and testing of active contour model for mass shape refinement.

### **(D) Develop deformable object boundary models for boundary refinement and second stage segmentation (Task 8)**

Although initial mass segmentation resulted in reasonable mass shapes for most of the masses, further refinement was necessary before detection and segmentation of the spiculations. We have developed an active contour model for mass shape refinement.

An active contour is a deformable continuous curve, whose shape is controlled by internal forces (the model, or a-priori knowledge about the object to be segmented) and external forces (the image)[9]. The internal forces impose a smoothness constraint on the contour, and the external forces push the contour towards salient image features, such as edges. To solve a segmentation problem, an initial boundary is iteratively deformed so that the energy due to internal and external forces is minimized along the contour.

The internal energy components in our active contour model were the continuity and curvature of the contour, as well as the homogeneity of the segmented object. The external energy components were the negative of the smoothed image gradient magnitude, and a balloon force that exerts pressure at a normal direction to the contour. The contour was represented by the vertices of an  $N$ -point polygon whose vertices were  $v(i)=(x(i),y(i))$ ,  $i=1,\dots,N$ . The energy to be minimized was defined as

$$E = \sum_{i=1}^N [w_{curv} E_{curv}(i) + w_{cont} E_{cont}(i) + w_{grad} E_{grad}(i) + w_{bal} E_{bal}(i)] + w_{hom} E_{hom} \quad (1)$$

where each energy term has a weight,  $w$ . The definition and purpose of the energy terms are described next.

The curvature energy term is approximated by the second derivative of the contour,  $E_{curv}(i) = |\mathbf{v}(i-1) - 2\mathbf{v}(i) + \mathbf{v}(i+1)|$ . This term is large when the angle at vertex  $i$  is small. By discouraging small angles at vertices, this term attempts to smooth the contour. The continuity term,  $w_{cont} E_{cont}(i)$ , is represented by the deviation of the length of the line segment under consideration from the average line segment length  $\bar{d}$ . Therefore this term maintains the approximately regular spacing between the vertices along the contour. The image gradient magnitude is obtained by smoothing the image with a low-pass filter, finding the partial derivatives in the horizontal and vertical directions, and then computing the magnitude of the partial derivative vector. Since the gradient energy,  $E_{grad}(i)$ , is defined as the negative of the gradient magnitude, minimizing this term attracts the contour to image edges. The effect of the balloon energy,  $E_{bal}(i)$ , can best be understood by considering how the moving the vertex  $i$  from  $\mathbf{v}(i)$  to  $\mathbf{v}'(i)$  affects this energy component. The normal direction to the contour at vertex  $i$  is defined as the average of the normals to the lines joining vertex  $i$  to vertices  $i-1$  and  $i+1$ . The balloon energy is defined as the cosine of the angle between this normal vector and the vector  $\mathbf{v}'(i) - \mathbf{v}(i)$ , which is the movement vector of vertex  $i$ . If the weight term  $w_{bal}$  is positive, then this energy component encourages the contour to expand in the normal direction. This term is required to prevent the contour from collapsing onto itself, which is a well-known phenomenon in active contour models [10]. The purpose of the homogeneity term,  $w_{hom} E_{hom}(i)$ , is to make the object and the background regions defined by the contour as homogeneous as possible within each region, and to maximize the difference between the two regions. The size of the background region in our model is defined to be the same as that of the object, so that only a relatively small neighborhood around the object is considered as the background. The homogeneity energy is defined as the ratio of within-region sum-of-squares and between-region sum-of-squares, where the two regions are the object and the background regions. In an image where both the object and the background have uniform and different gray-level values, the homogeneity energy will be zero when the contour is optimized. If the contour is not optimized, then both the background and the object will be less homogeneous, and the contour can be improved to reduce the homogeneity energy.

To minimize the contour energy, we used a greedy algorithm that was first proposed by Williams and Shah [11]. In this algorithm, the contour was iteratively optimized starting with the initial contour provided by the output of the first stage segmentation. At each iteration, a neighborhood of each vertex was examined, and the vertex was moved to the location that minimizes the contour energy. The algorithm stopped when there was no movement of the vertices, or when all the vertices of the contour were at locations already visited at a previous iteration.

### (E) Obtaining hand drawn mass boundaries from radiologists and evaluation of segmentation accuracy (Task 9)

For an evaluation of the segmentation technique we compared the computer segmentations with hand segmentations using the expertise of the radiologist.

### **Obtaining hand drawn mass boundaries from radiologists**

An MQSA-approved radiologist experienced in breast imaging outlined the mass boundaries of the masses on 239 ROIs using an interactive image analysis tool on a UNIX workstation.

In the future year more MQSA-approved radiologists experienced in breast imaging will hand segment mass boundaries of the masses on the ROIs.

### **Formulate quantitative measures for assessing segmentation accuracy**

For the purpose of our accuracy analysis, the radiologists hand segmentations were used to compare with the computer segmentations. Three quantitative measures were used for evaluation of the accuracy of the computer segmentations: Hausdorff distance, average Hausdorff distance and the area overlap measure.

Hausdorff distance between two curves is defined as the maximum of the closest point distances (DCPs) between the two curves [12], [13]. The closest point distance (DCP) associates each point on both curves to a point on the other curve, and the Hausdorff distance finds the largest distance between the associated points.

The average Hausdorff distance on the other hand finds the average of the DCPs between the two curves.

Area overlap is defined as follows:

$$A_{overlap} = \frac{A_1 \cap A_2}{A_1 \cup A_2} 100,$$

where  $A_1$  is area inside the hand segmented mass outline and  $A_2$  is area inside the computer segmented mass outline.

### **Evaluate quantitatively the accuracy of computer boundary segmentation using radiologists hand segmentation**

All results presented in the following are average results for the 239 ROIs.

The results of the first stage of segmentation by the K-means clustering algorithm are the following: average area overlap of 40%, average Hausdorff distance of 5.58mm, and average Hausdorff distance of 2.19mm averaged over 239 ROIs.

The results of the active contour segmentation are the following: average Area overlap of 67%, average Hausdorff distance of 4.49mm, and average Hausdorff distance of 1.27mm averaged over 239 ROIs.

The active contour segmentation improved the segmentation accuracy. The above results confirm the visual satisfactory agreement between the active contour segmentation and radiologist hand segmentation.

In the future year the quality of the computer segmentation will also be estimated by means of qualitative observer study.

### **(F) Develop methods for extracting morphological and texture features from masses segmented from ROIs extracted from current and prior mammograms (Task 10)**

The texture features used in this study were calculated from run-length statistics (RLS) matrices [14]. The RLS matrices were computed from the images obtained by the rubber band straightening transform (RBST)[15]. The RBST maps a band of pixels surrounding the mass onto the Cartesian plane (a rectangular region). In the transformed image, the mass border appears approximately as a horizontal edge, and spiculations appear approximately as vertical lines.

RLS texture features were extracted from the vertical and horizontal gradient magnitude images, which were obtained by filtering the RBST image with horizontally or vertically oriented Sobel filters and computing the absolute gradient values of the filtered image. Five texture measures, namely, short run emphasis, long run emphasis, gray level nonuniformity, run length nonuniformity, and run percentage were extracted from the vertical and horizontal gradient images in two directions,  $\theta = 0^\circ$ , and  $\theta = 90^\circ$ . Therefore, a total of 20 RLS features were calculated for each ROI. The definition of the RLS feature measures can be found in the literature [14].

The morphological features were extracted from the automatically segmented mass shape. Five of morphological features were based on the normalized radial length (NRL), defined as the Euclidean distance from the object's centroid to each of its edge pixels, i.e., the radial length, and normalized relative to the maximum radial length for the object [16]. The following five NRL features were extracted: mean, standard deviation, entropy, area ratio, zero crossing count. In addition, the perimeter, area, circularity, rectangularity, contrast, perimeter-to-area ratio and Fourier descriptor were extracted. The detailed definition of the morphological features can be found in [17], [18].

A spiculation measure was defined for each pixel on the mass border by using the statistics of the image gradient direction relative to the normal direction to the mass border in a ring of pixels surrounding the mass [17], [19]. The spiculation measure for each border pixel was normalized to be between 0 and  $\pi/2$ , with a value of  $\pi/4$  indicating a random orientation of image gradients, and larger values indicating a higher likelihood of spiculation. Three features were extracted from the spiculation measure. The first feature was the average of the spiculation measure for all pixels on the mass boundary. The second feature was the percentage of border pixels with a spiculation measure larger than  $\pi/4$ , and the third feature was the average of the spiculation measure for those pixels with a spiculation measure larger than  $\pi/4$ .

A total of 35 features (20 RLS, 12 morphological and 3 spiculation) were therefore extracted from each ROI.

#### **(G) Analyze techniques for characterizing differences in these features (Task 11)**

Additionally, difference features were obtained by subtracting a prior feature from the corresponding current feature. Therefore, 35 difference features were derived from the 20 RLS, 12 morphological and 3 spiculation features.

We are in a process of design of a new classification scheme allowing direct merge of current and prior information. The input feature space to the classifier will include the current, prior and difference features. This will allow the classifier to choose the individual current and prior features or the difference features. Stepwise feature selection with simplex optimization will be used to select the optimal feature subset. A linear discriminant classifier (LDA) and neural network classifiers will be used to merge the selected features for classification of malignant and benign masses. A leave-one-case-out training and testing resampling scheme will be used for feature selection and classification.

We have presented preliminary results on this method at the RSNA meeting [20] and SPIE meeting [21].

## (7) Conclusion

During this year, we have continued the development of the regional registration technique. The density-weighted contrast enhancement (DWCE) technique improves the localization of the corresponding mass on the prior mammogram. 179 temporal pairs of mammograms containing biopsy-proven masses were used for evaluation. Eighty-four percent of the estimated lesion locations resulted in an area overlap of at least 50% with the true lesion locations. The average distance between the estimated and the true centroids of the lesions on the prior mammogram was  $4.8 \pm 6.9$  mm. The registration accuracy of the current method has been improved in comparison with that without DWCE. This result indicates that our technique is a promising approach for identification of corresponding lesions on temporal pairs of mammograms and thus may be used as a basis for analysis of interval change on mammograms. We will continue to enlarge the data set and improve the registration method in future year.

Two hundred thirty nine regions of interest containing the corresponding masses were identified by MQSA radiologist on the current and prior mammograms of the temporal pair. The masses were automatically segmented using a K-means clustering algorithm and active contour model. Additionally, hand drawn mass boundaries from radiologists were obtained and used for evaluation of segmentation accuracy. The initial mass segmentation by the K-means clustering algorithm was satisfactory (average area overlap of 40%, average Hausdorff distance of 5.58mm, and average Hausdorff distance of 2.19mm averaged over 239 ROIs). The active contour model further improved the accuracy of mass segmentation (average Area overlap of 67%, average Hausdorff distance of 4.49mm, and average Hausdorff distance of 1.27mm averaged over 239 ROIs ). The active contour model showed to be useful for precise mass segmentation.

A total of 35 features (20 texture, 12 morphological and 3 spiculation) were extracted from each mass. Additional difference features were obtained by subtracting the features of the prior mass from those of the current mass. Therefore, 35 difference features were derived from the 20 texture, 12 morphological and 3 spiculation features. The feature space for each temporal pair consisted of the texture, spiculation and morphological features from both the prior and the current mammograms and the difference features. The obtained features will be used for classification of malignant and benign temporal masses as well as detection of temporal change.

We are in a process of design of a new classification scheme allowing direct merge of current and prior information. The input feature space to the classifier will include the current, prior and difference features. This will allows the classifier to choose the individual current and prior features or the difference features in order to obtain the best combination and merge of the features for high classification accuracy and optimal detection of interval change.

Further study is underway to develop a feature matching method to improve lesion localization within the search region. We will continue the development of automated method to extract and analyze features extracted from corresponding masses on a temporal pair of mammograms for analysis of the temporal changes.

## (8) References

- [1] H. C. Zuckerman, "The role of mammography in the diagnosis of breast cancer," in *Breast Cancer, Diagnosis and Treatment*, edited by I. M. Ariel and J. B. Cleary (McGraw-Hill, New York, 1987), pp. 152-172.

- [2] C.C. Boring, T. S. Squires, T. tong and S. Montgomery, "Cancer statistics 1994", *CA-A Cancer Journal for Clinicians* 44, 7-26, 1994.
- [3] S.S. Gopal, H.P. Chan, T.E. Wilson, M.A. Helvie, N. Petrick, B. Sahiner, "A regional registration technique for automated interval change analysis of breast lesions on mammograms", *Medical Physics*, 1999, 26:2669-2679.
- [4] L. Hadjiiski, H.P. Chan, B. Sahiner, N. Petrick, M.A. Helvie, S.S. Gopal, "Automated identification of breast lesions in temporal pairs of mammograms for interval change analysis", Presented at the 85<sup>th</sup> *Scientific Assembly and Annual Meeting of the Radiological Society of North America*, Nov.28-Dec.3, 1999, Chicago, Illinois. *Radiology* 1999; 213(P): 229-230.
- [5] L. Hadjiiski, H.P. Chan, B. Sahiner, N. Petrick, M.A. Helvie, S. Paquerault, C. Zhou, "Interval Change Analysis in Temporal Pairs of Mammograms Using a Local Affine Transformation", Poster Presentation at *SPIE International Symposium on Medical Imaging*, San Diego, California, February 12-18, 2000., *Proc. SPIE Medical Imaging, 2000*, 3979, pp.847-853.
- [6] L. Hadjiiski, H.P. Chan, B. Sahiner, N. Petrick, M. Helvie, "Automated Registration of Breast Lesions in Temporal Pairs of Mammograms for Interval Change Analysis – Local Affine Transformation for Improved Localization", *Medical Physics*, June 2001 (in press).
- [7] L. Hadjiiski, N. Petrick, H.P. Chan, B. Sahiner, M. A. Helvie, C. Zhou, M. Gurcan, S. Paquerault, "Regional registration of masses on current and prior mammograms using DWCE segmentation", Presented at *The World Congress on Medical Physics and Biomedical Engineering*, Chicago, July 23 - 28, 2000.
- [8] B. Sahiner, H. P. Chan, N. Petrick, D. Wei, M. A. Helvie, D. D. Adler, and M. M. Goodsitt, "Image feature selection by a genetic algorithm: Application to classification of mass and normal breast tissue on mammograms," *Med. Phys.* 23, 1671-1684 (1996).
- [9] M. Kass, A. Witkin, and D. Terzopoulos, "Snakes: active contour models," *Int. J. Comput. Vision* 1, 321-331 (1987).
- [10] L. D. Cohen, "On active contour models and balloons," *CVGIP: Image Understanding* 53, 211-218 (1991).
- [11] D. J. Williams and M. Shah, "A fast algorithm for active contours and curvature estimation," *CVGIP: Image Understanding* 55, 14-26 (1992).
- [12] D.P. Huttenlocher, G.A. Klanderman and W.J. Ruclidge, "Comparing images using the Hausdorff distance", *IEEE Trans. Pattern Anal. Mach. Int.* 15, 850-863 (1993).
- [13] V. Chalana and Y.Kim, "A methodology for evaluation of image segmentation algorithms on medical images", *Proc. SPIE* 2710, 178-189 (1996).
- [14] M. M. Galloway, "Texture classification using gray level run lengths," *Comp. Graph. Img Proc.* 4, 172-179 (1975).
- [15] B. Sahiner, H. P. Chan, N. Petrick, M. A. Helvie, and M. M. Goodsitt, "Computerized characterization of masses on mammograms: The rubber band straightening transform and texture analysis," *Med. Phys.* 25, 516-526 (1998).
- [16] J. Kilday, F. Palmieri, and M. D. Fox, "Classifying mammographic lesions using computer-aided image analysis," *IEEE Trans. Med. Img.* 12, 664-669 (1993).
- [17] B. Sahiner, H.-P. Chan, N. Petrick, M. A. Helvie, and L. M. Hadjiiski, "Improvement of mammographic mass characterization using spiculation measures and morphological features," *Med. Phys.* (submitted), (2000).
- [18] N. Petrick, H. P. Chan, B. Sahiner, and M. A. Helvie, "Combined adaptive enhancement and region-growing segmentation of breast masses on digitized mammograms," *Med. Phys.* 26, 1642-1654 (1999).

- [19] B. Sahiner, H. P. Chan, N. Petrick, L. M. Hadjiiski, M. A. Helvie, and S. Paquerault, "Active contour models for segmentation and characterization of mammographic masses," The 5th International Workshop on Digital Mammography Proc. IWDM-2000, (in press) (2000).
- [20] L. Hadjiiski, B. Sahiner, H.P. Chan, N. Petrick, M.A. Helvie, M. Gurcan, "Computer-Aided Classification of Malignant and Benign Breast Masses by Analysis of Interval Change of Features in Temporal Pairs of Mammograms", Presented at the 86<sup>th</sup> *Scientific Assembly and Annual Meeting of the Radiological Society of North America (RSNA)*, Chicago, Illinois, November 26 - December 1, 2000. *Radiology* 2000; 217(P): 435.
- [21] L. Hadjiiski, B. Sahiner, H.P. Chan, N. Petrick, M.A. Helvie, M. Gurcan, "Analysis of Temporal Change of Mammographic Features for Computer Aided Characterization of Malignant and Benign Masses", Presented at the *SPIE International Symposium on Medical Imaging*, San Diego, California, February 17-22, 2001. To appear in *Proc. SPIE Medical Imaging 2001*.

## (9) Appendix

### 1. Key research accomplishments in current year as a result of this grant

- Database collection and extraction of regions of interest (Task 1).
- Further developments of methods for establishing corresponding locations in current and previous mammograms (Task 3).
- Identify technique to be used in the first stage of segmentation (Task 7).
- Develop deformable object boundary models for boundary refinement and second stage segmentation (Task 8).
- Obtaining hand drawn mass boundaries from radiologists and evaluation of segmentation accuracy (Task 9).
- Develop methods for extracting morphological and texture features from masses segmented from ROIs extracted from current and prior mammograms (Task 10).
- Analyze techniques for characterizing differences in these features (Task 11).

### 2. Publications in current year as a result of this grant

- [1] L. Hadjiiski, H.P. Chan, B. Sahiner, N. Petrick, M. Helvie, "Automated Registration of Breast Lesions in Temporal Pairs of Mammograms for Interval Change Analysis – Local Affine Transformation for Improved Localization", *Medical Physics*, June 2001 (in press).
- [2] L. Hadjiiski, H.P. Chan, B. Sahiner, N. Petrick, M.A. Helvie, S. Paquerault, C. Zhou, "Interval Change Analysis in Temporal Pairs of Mammograms Using a Local Affine Transformation", Poster Presentation at *SPIE International Symposium on Medical Imaging*, San Diego, California, February 12-18, 2000., *Proc. SPIE Medical Imaging, 2000, 3979, pp.847-853*.
- [3] Hadjiiski L, Chan HP, Sahiner B, Petrick N, Helvie MA. "Interval change analysis in temporal pairs of mammograms using an automated registration technique". **Oral presentation** at the *Era of Hope Meeting, U. S. Army Medical Research and Materiel Command, Department of Defense, Breast Cancer Research Program*, Atlanta, Georgia, June 8-12, 2000., *Proc. Era of Hope Meeting 2000, pp.247*.
- [4] Hadjiiski L, Chan HP, Sahiner B, Petrick N, Helvie MA. Interval change analysis in temporal pairs of mammograms using an automated registration technique. **Poster presentation** at the *Era of Hope Meeting, U. S. Army Medical Research and Materiel Command, Department of Defense, Breast Cancer Research Program*, Atlanta, Georgia, June 8-12, 2000.
- [5] L. Hadjiiski, N. Petrick, H.P. Chan, B. Sahiner, M. A. Helvie, C. Zhou, M. Gurcan, S. Paquerault, "Regional registration of masses on current and prior mammograms using DWCE segmentation", Presented at *The World Congress on Medical Physics and Biomedical Engineering*, Chicago, July 23 - 28, 2000.

- [6] L. Hadjiiski, B. Sahiner, H.P. Chan, N. Petrick, M.A. Helvie, M. Gurcan, "Computer-Aided Classification of Malignant and Benign Breast Masses by Analysis of Interval Change of Features in Temporal Pairs of Mammograms", Presented at the 86<sup>th</sup> *Scientific Assembly and Annual Meeting of the Radiological Society of North America (RSNA)*, Chicago, Illinois, November 26 - December 1, 2000. *Radiology* 2000; 217(P): 435.
- [7] L. Hadjiiski, B. Sahiner, H.P. Chan, N. Petrick, M.A. Helvie, M. Gurcan, "Analysis of Temporal Change of Mammographic Features for Computer Aided Characterization of Malignant and Benign Masses", Presented at the *SPIE International Symposium on Medical Imaging*, San Diego, California, February 17-22, 2001. To appear in *Proc. SPIE Medical Imaging 2001*.

**3. Copies of publications are enclosed with this report.**

## Monday, July 24, 2000 (continued)

- 3:00 pm MO-E301-04 Estimating Shoulder Maximum Muscle Forces in Individuals with C5-C6 Tetraplegia - A. Acosta \*, R. Kirsch
- 3:20 pm MO-E301-05 Effects of Triceps Surae Muscle Fatigue On Intrinsic and Reflex Contributions to Dynamic Ankle Stiffness - W. Qita, R. Kearney \*

-Room: 303

**MO-E303 Track 19: Medical physics curricula**

Chairs: Eduardo Galiano, Imater S.A., Asuncion, Paraguay and Basil Proimos, University of Patras, Patras, Greece

- 2:00 pm MO-E303-01 Medical Physics at the Adam Mickiewicz University, Poznań? - R. Krzyminiewski \*
- 2:20 pm MO-E303-02 Medical Physics Education and Training in Russia - O. Shereshevskiy \*
- 2:40 pm MO-E303-03 Improvement of Specialists Training On Medical Physics at the Moscow Engineering Physics Institute - V. Bolyatko \*, V. Klimanov
- 3:00 pm MO-E303-04 What Does Medical Physics Mean for a Small, Lesser Developed Nation; the Case of Paraguay - E. Galiano \*
- 3:20 pm MO-E303-05 The TEMPERE Project: A European Approach to the Training and Education of Medical Physicists and Biomedical Engineers - B. Proimos \*, C. Danciu, Z. Kolitsi, J. Horrocks, R. Speller, N. Pallikarakis, J. Barbenel

-Room: 305

**MO-E305 Track 01: Nuclear Imaging**

Chair: H Tang, University of California, San Francisco, CA

- 2:00 pm MO-E305-01 Development of Realistic Computer Generated Anthropomorphic Torso Phantoms for Medical Imaging - B. Tsui \*, W. Segars, K. LaCroix, D. Lalush
- 2:10 pm Student Paper Competition Finalist:  
MO-E305-02 Design, Development, and Implementation of a High Adaptability Whole Body Counting System - S. Steciw \*, L. Filipow
- 2:20 pm MO-E305-03 A Solid-State Intraoperative Beta Probe System - R. Raylman \*
- 2:30 pm MO-E305-04 CdZnTe Imaging Detectors for Nuclear Medicine - D. Wagenaar \*, M. Kalinosky, D. Burckhardt, J. Engdahl
- 2:40 pm MO-E305-05 Pixel-Pixel Interactions in a Square Pixel Array CdZnTe Detector - M. Kalinosky \*, D. Wagenaar, D. Burckhardt, J. Engdahl
- 2:50 pm MO-E305-06 A Comparison Between The Performance Of a Pixellated CdZnTe Based Gamma Camera and Anger NaI(Tl) Scintillator Gamma Camera - A. Amrami \*, G. Shani, y. Hefetz, I. Blevis, A. Pansky
- 3:00 pm MO-E305-07 Radionuclide Scatter Estimation Using EGS4-Generated Convolution Kernels - H. Tang \*, A. Da Silva, R. Hawkins, B. Hasegawa
- 3:10 pm MO-E305-08 Effects of Scatter Correction in Quantitative Cardiac SPECT Studies Reconstructed Using Consistency Conditions - A. da Silva \*, A. Furlan, C. Robilotta
- 3:20 pm MO-E305-09 An Iterative Transmission Algorithm Incorporating Cross-Talk Correction for SPECT - M. Narayanan \*, M. King, C. Byrne
- 3:30 pm MO-E305-10 Image Reconstruction for the YAPPET Tomograph Using a Fast OS-EM Algorithm - A. Motta, G. Di Domenico, G. Zavattini, C. Damiani, A. Del Guerra \*

## Monday, July 24, 2000 (continued)

-Room: 307

**MO-E307 Track 01: Mammography Computer Aided Diagnosis**

Chair: Heang-Ping Chan, University of Michigan, Ann Arbor, MI

- 2:00 pm MO-E307-01 Multiple Benefits of Computer-Aided Diagnosis (CAD) in the Diagnosis of Malignant and Benign Breast Lesions - Y. Jiang \*, R. Nishikawa, R. Schmidt, C. Metz, K. Doi
- 2:10 pm MO-E307-02 Regional Registration of Masses On Current and Prior Mammograms Using DWCE Segmentation - L. Hadjiiski \*, N. Petrick, H. Chan, B. Sahiner, M. Helvie, C. Zhou, M. Gurcan, S. Paquerault
- 2:20 pm MO-E307-03 Robustness of Computer-Extracted Features Used in Mass Detection - A. Baehr \*, M. Giger, M. Kupinski, K. Yao, L. Venta, C. Vyborny
- 2:30 pm MO-E307-04 Detection of Mass Lesions in Mammography Using Feature-Filtering Techniques - M. Kupinski \*, M. Giger
- 2:40 pm MO-E307-05 Computer Classification of Mass Lesions On Small-Field Digital Mammography - M. Maloney \*, M. Giger, Z. Huo, L. Venta, M. Kupinski
- 2:50 pm MO-E307-06 Differences in Computer Aided Diagnosis of Breast Cancer: Masses Vs. Calcifications - M. Markey \*, J. Lo, C. Floyd
- 3:00 pm MO-E307-07 Fully Automated Computer-Aided Diagnosis (CAD) System for Microcalcifications On Digital Mammograms - J. Vargas \*, Y. Jiang, R. Nishikawa, J. Papaioannou, H. Yoshida
- 3:10 pm MO-E307-08 Eliminating False-Positive Microcalcification Detections in a Mammography CAD Scheme Using a Bayesian Neural Network - D. Edwards \*, M. Kupinski, R. Nagel, R. Nishikawa, J. Papaioannou
- 3:20 pm MO-E307-09 The CALMA Database of Mammographic Images: Search for Spiculated Lesions and Microcalcification Clusters - U. Bottigli, R. Palmiero, E. Pernigotti, M. Reggiani, V. Rosso, S. Tangaro, O. Venier, S. Amendiolia, A. Ceccopieri, M. Ciocci, P. Delogu, G. Dipasquale, M. Fantacci, P. Maestro, A. Marchi, P. Oliva, A. Stefanini, S. Stumbo, M. Bisogni, V. Marzulli, V. Marzulli \*
- 3:30 pm MO-E307-10 The Detection of Lesions in Scintimammograms Through Morphological Filters - C. Costa Fo \*, M. Costa, L. Moura

-Room: 309

**MO-E309 Track 02: Brachytherapy 1**

Chairs: Robert Zwicker, Richmond, VA and Jeffrey Williamson, Radiation Oncology Center, Washington University, St. Louis, MO

- 2:00 pm MO-E309-01 Dual Energy CT Tissue Quantification for Monte-Carlo Based Treatment Planning for Brachytherapy - S. Devic, J. Monroe, S. Mutic, B. Whiting, J. Williamson \*
- 2:10 pm MO-E309-02 On the Dosimetric Influences of Air-Kerma Strength Calibration Geometry and Internal Source Structure for <sup>103</sup>Pd and <sup>125</sup>I Brachytherapy Sources - J. Williamson \*
- 2:20 pm MO-E309-03 Accelerated Monte Carlo-Based Dose Calculations for Brachytherapy Planning Using Correlated Sampling - H. Hedtjarn \*, G. Alm Carlsson, J. Williamson
- 2:30 pm MO-E309-04 Dosimetric Characterization of a New <sup>125</sup>Iodine Brachytherapy Source, Model I125-SL - R. Wallace \*

## **Regional Registration of Masses On Current and Prior Mammograms Using DWCE Segmentation**

L Hadjiiski\*, N Petrick, HP Chan, B Sahiner, M Helvie, C Zhou, M Gurcan, S Paquerault, The University of Michigan, Ann Arbor, Michigan, U.S.A, Department of Radiology, University of Michigan, Ann Arbor, MI 48109, USA

**Scientific Session:** *MO-E307-02* Mammography Computer Aided Diagnosis

**Track:** 01 Diagnostic Physics, Medical Imaging, and Image Processing

We are developing a computerized method to analyze interval change of mammographic lesions. In this study, we investigated the use of the density-weighted contrast enhancement (DWCE) technique to improve the localization of the corresponding mass on the prior mammogram.

A regional registration technique was developed for identifying masses on temporal pairs of mammograms. The breast images from the current and prior mammogram were first aligned globally based on the mutual information. An initial fan-shape search region was defined on the prior mammogram using a polar coordinate system with the origin at the nipples. The location of the fan-shaped region was refined by affine transformation and simplex optimization. The DWCE technique was then used to segment dense structures within the search region. A search for the best match between the lesion template from the current mammogram and a structure on the prior mammogram was performed within the DWCE segmented densities. The technique was evaluated on 124 temporal pairs of mammograms containing biopsy-proven masses. The true corresponding mass location on the prior mammogram was identified by an experienced radiologist. It was found that 85% of the estimated mass locations resulted in an area overlap of at least 50% with the true mass locations. The average distance between the estimated and the true centroid of the lesions on the prior mammogram was 2.6mm (std 2.1mm) for this subset and was 4.7mm (std 6.2mm) over the entire data set. The DWCE segmentation improved the accuracy of matching by directing the search to the dense structures and thus reducing the chance of mismatch.

## **INTERVAL CHANGE ANALYSIS IN TEMPORAL PAIRS OF MAMMOGRAMS USING AN AUTOMATED REGISTRATION TECHNIQUE**

**Lubomir Hadjiiski, Heang-Ping Chan, Berkman Sahiner, Nicholas Petrick,  
Mark A. Helvie**

Department of Radiology, The University of Michigan,  
Ann Arbor, MI 48109-0904

E-mail: lhadjisk@umich.edu

The aim of this study is to develop a registration technique for automated identification of corresponding lesion on a prior mammogram. This technique is the basis for interval change analysis of breast lesions in computer-aided diagnosis applications.

A multistage regional registration technique was developed for identifying corresponding masses on temporal pairs of mammograms. It combined both a global and a local alignment procedure. In the first stage, the breast images from the current and prior mammograms were globally aligned. An initial fan-shape search region was then defined on the prior mammogram based on the mass location on the current mammogram. In the local alignment stage, the location of the search region on the prior mammograms was first refined by maximizing a correlation measure between a template extracted from the current mammogram and the breast structures on the prior mammogram. The affine transformation in combination with simplex optimization was then employed to warp this local region. This alignment step further improved the match between the regions on the current and prior mammograms by correcting for local geometric distortions due to differences in positioning of the breast and in breast compression. In the final stage a search for the best match between the lesion template from the current mammogram and a structure on the prior mammogram was carried out within the refined search region. This technique was evaluated on 107 temporal pairs of mammograms containing biopsy-proven masses. The true lesion locations were identified by an MQSA-certified radiologist on all mammograms. The accuracy of the multistage regional registration was analyzed by evaluating the overlap area between the estimated and the true lesions on the prior mammograms as well as the average distance between the centroids of the estimated and true lesion locations.

In this study 88% of the estimated lesion locations resulted in an area overlap of at least 50% with the true lesion locations. The average distance between the estimated and the true centroid of the lesions on the prior mammogram was  $4.3 \pm 4.9$  mm over all cases.

The multistage regional registration technique is useful for identifying corresponding lesions on temporal pairs of mammograms. Local warping based on the affine transformation improves the accuracy of identification.

The U.S. Army Medical Research and Materiel Command under DAMD17-98-1-8211 supported this work.

percentage patient-related working time were somewhat mis-judged by the radiologists. After correction for the differences found between the survey and the observation, the average workload was estimated to be 53.4 hours a week per fte, with 73% spent on patient-related activities. The Dutch radiologists performed 12.243 procedures a year per fte in 1998. U.S. radiologists reported an average of 51.3 hours a week per fte in 1995, with 89% of the working time spent on patient-related activities. They performed 11.600 procedures a year per fte in 1995.

**CONCLUSIONS:** The workload of Dutch radiologists is roughly comparable with the workload of U.S. radiologists. (This research project was supported by the Dutch Radiology Society.)

## Wednesday Morning • Room S401AB

### Physics (CAD: Mammography and Pulmonary)

In joint sponsorship with the American Association of Physicists in Medicine

**PH**  
PRESIDING: **Carey E. Floyd, Jr, PhD**, Durham, NC  
Computer Code: K02 • 1½ hours

To receive credit, relinquish attendance voucher at end of session.

#### 961 • 10:00AM

##### Mammographic Parenchymal Patterns as Predictors for Breast Cancer Risk

Z. Huo, PhD, Chicago, IL • M.L. Giger, PhD • W. Zhong, MS • R.M. Nishikawa, PhD • D.E. Wolverton, MD • O.I. Olopade, MD

**PURPOSE:** To identify radiographic markers for breast cancer risk prediction.

**METHOD AND MATERIALS:** Mammograms from 503 women (380 with no cancer, 30 with BRCA1/BRCA2 gene mutation and 93 with breast cancer) were digitized at a pixel size of 0.1 mm and 10-bit quantization. Fourteen computer-extracted features, including skewness, coarseness, contrast and RMS variation were calculated from the central region of breast image to characterize percent dense of the breast or the heterogeneity (diffuse) patterns in the dense portions of the breast. Three different approaches were employed to relate these features to risk of developing breast cancer: 1) to distinguish mammographic patterns seen in low-risk women from those who inherited a mutated form of the BRCA1/BRCA2 gene, which confers a very high risk of developing breast cancer; 2) to correlate with clinical risk models (Gail and Claus models), which use well-known epidemiological factors such as age, family history of breast cancer, and reproductive history, and 3) to differentiate mammographic patterns seen in cancer-free women and in women who have breast cancer. Stepwise linear discriminant analysis, stepwise linear regression and stepwise linear logistic regression were employed to identify features that were useful in differentiating between the "low-risk" and "high-risk" women described in each of the three approaches, respectively.

**RESULTS:** Similar computer-extracted mammographic features were identified from the three different approaches. Results from all three approaches suggest that women at high risk of developing breast cancer tend to have dense breasts and their mammographic patterns tend to be coarse and low in contrast. Linear discriminant analysis yielded  $A_z$  of 0.89 in differentiating between BRCA1/BRCA2 mutation carriers and low-risk women. Linear regression on the selected computer-extracted features and age achieved correlation coefficients ( $r$ ) of 0.57 and 0.61 in predicting the risks as determined from the Gail and Claus models, respectively. Linear logistic regression on the selected computer-extracted features and age yielded a correlation coefficient of 0.82 (pseudo) in predicting breast cancer risk.

**CONCLUSIONS:** Mammographic patterns characterized by computer-extracted mammographic features may be potentially used as predictors for breast cancer risk. (ZH, MLG, and RMN are shareholders of R2 Technology, Inc., Los Altos, CA.)

#### 962 • 10:09AM

##### Computer-aided Estimation of Mammographic Breast Density

C. Zhou, PhD • H. Chan, PhD, Ann Arbor, MI • M.A. Helvie, MD • N.A. Petrick, PhD • M.M. Goodsitt, PhD • B. Sahiner, PhD

**PURPOSE:** Studies indicate that mammographic density is correlated with breast cancer risk. Current methods use visual judgment or manual segmentation to estimate the percentage of dense area on mammograms. We are developing an image analysis method to automatically estimate mammographic breast density.

**METHOD AND MATERIALS:** A mammogram is digitized and the pixels are averaged to 0.8 mm. The breast region is first segmented by an automated boundary tracking and a pectoral muscle trimming algorithm. An adaptive dynamic range reduction technique is used to reduce the low frequency background and to enhance the characteristic features of the gray level histogram. The breast images are classified into four classes according to the features of their gray level histograms by a rule-based classifier. For each class, a gray level threshold is automatically estimated to segment the dense tissue. The area of the segmented dense tissue as a percentage of the breast area is then calculated. The computer performance was compared to manual segmentation by 5 MQSA-approved radiologists. For each image, the radiologists provided a visual estimate as well as interactively selected a threshold for segmenting and computing the percent dense area.

**RESULTS:** In this preliminary study, four-view mammograms from 65 patients were used. The breast boundary was accurately tracked on 92.3% ( $N=240$ ) of the mammograms, and the pectoral muscle was correctly trimmed on 74.6% of the MLO views. The histograms of 6% (8 CC and 8 MLO views) of the breast regions did not exhibit the typical characteristic features of the four classes and were misclassified by the computer, resulting in poor segmentation of the dense region. For the CC-views with correct classification, the correlation between the computer's estimated percent dense area and the radiologists' manual segmentation, averaged over 5 radiologists, was 0.94, and between the computer and the radiologists' average visual estimate was 0.87. These correlations were 0.91 and 0.82, respectively, for the MLO-views with correct classification.

**CONCLUSIONS:** The results demonstrate the feasibility of developing an automated image analysis technique for mammographic density estimation although the accuracy of the different image processing stages still needs to be improved. Computerized analysis reduces the interobserver and intraobserver variabilities of the current approach. The consistency and reproducibility are important for risk estimation or for monitoring breast density change in a prevention or intervention program.

#### 963 • 10:18AM

##### Computer-aided Classification of Malignant and Benign Breast Masses by Analysis of Interval Change of Features in Temporal Pairs of Mammograms

L.M. Hadjiiski, PhD, Ann Arbor, MI • H. Chan, PhD • B. Sahiner, PhD • N.A. Petrick, PhD • M.A. Helvie, MD • M.N. Gurcan, PhD

**PURPOSE:** To develop a computer-aided diagnosis method to assist radiologists in analysis of interval changes of corresponding masses on a temporal pair of mammograms.

**METHOD AND MATERIALS:** An automated method was developed to extract and analyze features extracted from corresponding masses on a temporal pair of mammograms. Regions of interest containing the corresponding masses were identified on the current and prior mammograms of the temporal pair. The masses were automatically segmented using an active contour model. 20 Run Length Statistics (RLS) features, 3 spiculation features, and mass size were extracted from each mass. An additional 20 difference RLS features were obtained by subtracting the RLS features of the prior mass from those of the current mass for each temporal pair. The feature space for each temporal pair consisted of the RLS and spiculation features from both the prior and the current mammograms and the difference RLS features. Stepwise feature selection with simplex optimization was used to select the optimal feature subset. A linear discriminant classifier (LDA) was used to merge the selected features for classification of malignant and benign masses. In this study, 93 temporal image pairs from 38 patients containing biopsy-proven masses on the current mammograms were chosen from patient files. The true mass locations were identified by an experienced radiologist on all mammograms. All cases were selected from a biopsy database so that interval change was observed for most of the masses even if they were found to be benign after biopsy. This was therefore a difficult data set for interval change analysis. A leave-one-case-out training and testing resampling scheme was used for feature selection and classification. The classification accuracy was analyzed by receiver operating characteristic (ROC) methodology.

**RESULTS:** An average of 9 features was selected from the 37-training subsets. The selected features included 3 difference RLS features, 3 RLS and 1 spiculation features from the current image, and 2 spiculation features from the prior. The classifier achieved a training  $A_z$  of 0.92 and a test  $A_z$  of 0.82.

**CONCLUSIONS:** The size of the mass is not a useful feature for difficult cases because many benign masses grow over time. The difference RLS and prior spiculation features are useful for identification of malignancy in temporal pairs of mammograms. Further studies are underway to improve the technique and to evaluate the performance on a larger data set.

was reduced to 6.3FPs/image at 96% sensitivity by rule-based classification of single view features. Further FP reduction in single view resulted in 1.9 FPs/image at 80% sensitivity and 1.1 FPs/image at 70% sensitivity. By combining single-view detection with the correspondence classifier, detection accuracy improved to 1.5 FPs/image at 80% sensitivity and 0.7 FPs/image at 70% sensitivity. Our results indicate that the correspondence of geometric, morphological, and textural features of a mass on two different views provides valuable additional information for reducing FPs.

#### 4322-70, Session 12

##### Computer-Aided Diagnosis of Lesions on Multimodality Images of the Breast

Maryellen L. Giger, Karla Horsch, Zhimin Huo, Edward Hendrick, L. Venta, Carl J. Vyborny (University of Chicago, Department of Radiology, Chicago, IL 60637, Northwestern University, Department of Radiology, Chicago, IL)

The purpose of our study is to develop computerized methods for the analysis of lesions on multimodality images, i.e., from digitized mammograms and sonograms of the breast for aiding in the task of distinguishing between malignant and benign lesions. The overall computerized classification methods for mass lesions on digitized mammograms and sonograms include: (1) automatic lesion extraction, (2) automated feature extraction, and (3) automatic classification for merging the features into an estimate of the likelihood of malignancy. For the mammograms, computer-extracted lesion features include degree of spiculation, margin sharpness, lesion density, and lesion texture. For the ultrasound images, lesion features include margin definition, texture, shape, and posterior acoustic attenuation. On a database of 95 mammograms, the computer yielded an Az of 0.94 in the task of distinguishing between malignant and benign lesions. On a database of 169 ultrasound cases, the computer achieved an Az of 0.92 with a partial Az of 0.67. On a preliminary common database of 20 cases having both mammographic and ultrasound examinations, texture and margin information features performed best on the ultrasound image data yielding Az values of 0.91 and 0.80, respectively. The artificial neural network for the mammographic data yielded an Az value of 0.80.

#### 4322-71, Session 12

##### Analysis of Temporal Change of Mammographic Features for Computer-Aided Characterization of Malignant and Benign Masses

Lubomir Hadjiiski, Berkman Sahiner, Heang-Ping Chan, Nicholas Petrick, Mark A. Helvie, Metin Gurcan (Department of Radiology, The University of Michigan, Ann Arbor, MI 48109-0904)

A new classification scheme was developed to classify mammographic masses as malignant and benign by using interval change information. The masses on both the current and the prior mammograms were automatically segmented using an active contour method. From each mass, 20 run length statistics texture features (RLSF), 3 spiculation features (SPF), and mass size were extracted. Additionally, 20 difference RLSF were obtained by subtracting a prior RLSF from the corresponding current RLSF. The feature space consisted of the current RLSF, the difference RLSF, the current and prior SPF, and the current and prior mass sizes. Stepwise feature selection and linear discriminant analysis classification were used to select and merge the most useful features. A leave-one-case-out resampling scheme was applied to train and test the classifier using 140 temporal image pairs (85 malignant, 55 benign) obtained from 56 biopsy-proven masses (33 malignant, 23 benign). An average of 10 features were selected from the 56 training subsets: 4 difference RLSF, 4 RLSF and 1 SPF from the current image, and 1 SPF from the prior. The classifier achieved an average training Az of 0.92 and a test Az of 0.88. The information on the prior image significantly ( $p=0.01$ ) improved the accuracy for classification of the masses.

#### 4322-72, Session 12

##### Computer-Assisted Diagnosis of Chest Radiographs for Pneumoconioses

Peter Soliz, Marios S. Pattichis, Janakiraman Ramachandran, David S. James (PS Kestrel Corporation, 3815 Osuna Rd NE, Albuquerque, NM 87109) (MP, JR University of New Mexico, Electrical Engineering and Computer Engineering Dept., Albuquerque, New Mexico 87106) (DJ University of New Mexico Health Sciences Center, 2211 Lomas Blvd. NE, Albuquerque, NM 87131)

A Computer-assisted Chest Radiograph Reader System (CARRS) was developed for the detection of pathological features in lungs presenting with pneumoconioses. CARRS applies novel techniques in automatic image segmentation, incorporates neural networkbased pattern classification, and integrates these into a graphical user interface.

Three phases of CARRS are described: Chest radiograph quantization, rib and parenchyma segmentation, and classification. The quantization of the chest radiograph film was optimized to maximize the information content of the digital images. Entropy was used as the benchmark for optimizing the quantization.

The segmentation uses directional filters to enhance the anterior and posterior ribs. From the rib-segmented images, regions of interest were selected by the pulmonologist. A feature vector composed of image characteristics such as entropy, textural statistics, etc. was calculated. A laterally primed adaptive resonance theory (LAPART) neural network was used as the classifier. LAPART classification accuracy averaged 86.8%. "Truth" was determined by the two pulmonologists.

The CARRS has demonstrated potential as a screening device. Today, 90% or more of the chest radiographs seen by the pulmonologist are normal. A computer-based system that can screen 50% or more of the chest radiographs represents a large savings in time and dollars. Acknowledgement. NIOSH Grant 2R44 OHRRGM 03595

#### 4322-73, Session 12

##### Quantitative MR assessment of structural changes in white matter of children treated for ALL

Wilburn E. Reddick, John O. Glass, Raymond K. Mulhern (Department of Diagnostic Imaging and Behavioral Medicine, St. Jude Children's Research Hospital, Memphis, TN 38105-2794)

Our research builds on the hypothesis that white matter damage resulting from therapy spans a continuum of severity that can be reliably probed using non-invasive MR technology. This project focuses on children treated for ALL with a regimen containing seven courses of high dose methotrexate (HDMTX) which is known to cause leukoencephalopathy. Axial FLAIR, T1-, T2-, and PD-weighted images were acquired, registered and then analyzed with a hybrid neural network segmentation algorithm to identify normal brain parenchyma and leukoencephalopathy. Quantitative T1 and T2 maps were also analyzed at the level of the basal ganglia and the centrum semiovale. The segmented images were used as mask to identify regions of normal appearing white matter (NAWM) and leukoencephalopathy in the quantitative T1 and T2 maps. We assessed the longitudinal changes in volume, T1 and T2 in NAWM and leukoencephalopathy for 41 patients. The segmentation analysis revealed that 69% of patients had leukoencephalopathy after receiving seven courses of HDMTX. The leukoencephalopathy affected approximately 17% of the patients' white matter volume on average (range 2% - 38%). Relaxation rates in the NAWM were not significantly changed between the 1<sup>st</sup> and 7<sup>th</sup> courses. Regions of leukoencephalopathy exhibited a 13% elevation in T1 and a 37% elevation in T2 relaxation rates.

# Interval change analysis in temporal pairs of mammograms using a local affine transformation

Lubomir Hadjiiski, Heang-Ping Chan, Berkman Sahiner, Nicholas Petrick, Mark A. Helvie,  
Sophie Paquerault, Chuan Zhou

Department of Radiology, The University of Michigan, Ann Arbor, MI 48109-0904

## ABSTRACT

The aim of this study is to evaluate the use of a local affine transformation for computer-aided interval change analysis in mammography. A multistage regional registration technique was developed for identifying masses on temporal pairs of mammograms. In the first stage, the breast images from the current and prior mammograms were globally aligned. An initial fan-shape search region was defined on the prior mammogram. In the second stage, the location of the fan-shape region was refined by warping, based on an affine transformation and simplex optimization. A new refined search region was defined on the prior mammogram. In the third stage a search for the best match between the lesion template from the current mammogram and a structure on the prior mammogram was carried out within the search region. This technique was evaluated on 124 temporal pairs of mammograms containing biopsy-proven masses. Eighty-six percent of the estimated lesion locations resulted in an area overlap of at least 50% with the true lesion locations. The average distance between the estimated and the true centroid of the lesions on the prior mammogram was  $4.4 \pm 5.9$  mm. The registration accuracy was improved in comparison with our previous study that used a data set of 74 temporal pairs of mammograms. This improvement gain is mainly from the local affine transformation.

**Keywords:** Computer-Aided Diagnosis, Interval Changes, Affine Transform, Correlation, Mutual Information, Mammography, Malignancy

## 1. INTRODUCTION

Mammography is currently the most effective method for early breast cancer detection<sup>1,2</sup>. Analysis of interval changes is an important method used by radiologists to detect developing malignancy in mammographic interpretation<sup>3,4</sup>. A variety of computer-aided diagnosis (CAD) techniques have been developed to detect mammographic abnormalities and to distinguish between malignant and benign lesions. We are studying the use of CAD techniques to assist radiologists in interval change analysis.

Sallam *et al.*<sup>5</sup> have proposed a warping technique for mammogram registration based on manually obtained control points. A mapping function was calculated for mapping each point on the current mammogram to a point on the prior mammogram. Brzakovic *et al.*<sup>6</sup> have investigated a three-step method for comparison of most recent and prior mammograms. They first registered two mammograms using the method of principal axis, and partitioned the current mammogram using a hierarchical region-growing technique. Translation, rotation, and scaling were then used for registration of the partitioned regions. Vujovic *et al.*<sup>7</sup> have proposed a multiple-control-point technique for mammogram registration. They first determined several control points independently on the current and prior mammograms based on the intersection points of prominent anatomical structures in the breast. A correspondence between these control points was established based on a search in a local neighborhood around the control point of interest.

The previous techniques depend on the identification of control points. However, because the breast is mainly composed of soft tissue that can change over time, there are no obvious landmarks on mammograms. The crossing line structures are often fibrous tissue from different depths of the breast which overlap in a projection image. These crossing points are not invariant landmarks on the different mammograms. Because of the elasticity of the breast tissue, there is large variability in the positioning and compression used in mammographic examination. As a result, the relative positions of the breast tissues projected onto a mammogram vary from one examination to the other. Techniques that depend on identification of control points may not be generally applicable to registration of breast images.

Gopal *et al.*<sup>8,9,10</sup> and Hadjiiski *et al.*<sup>11</sup> have developed a multistage technique that defines a transformation to locally map the position of the mass on a current mammogram to that on the prior mammogram. A local search for the mass is then performed on the prior mammogram. Good *et al.*<sup>12</sup> also have developed a technique that defines a transformation to map all points from the current mammogram onto a prior mammogram. Then the current mammogram is subtracted from the prior mammogram.

The goal of our research is to develop a technique for computerized analysis of temporal differences between a lesion on the most recent mammogram and a prior mammogram of the same view. The computer algorithm will assist radiologists in quantifying interval changes and thus distinguishing between benign and malignant masses for CAD. In this study, we developed a local registration technique based on affine transformation and simplex optimization and evaluated its usefulness in improving the localization of the mass on the prior mammogram.

## 2. REGISTRATION TECHNIQUE

A multistage regional registration technique was developed for identifying corresponding masses on temporal pairs of mammograms. It combined both a global and a local alignment procedure. The block diagram of the regional registration technique is shown in Fig. 1. In the first stage, the breast images from the current and prior mammograms were globally aligned by maximizing a mutual information measure. An initial fan-shape search region was then defined on the prior mammogram based on the mass location on the current mammogram.

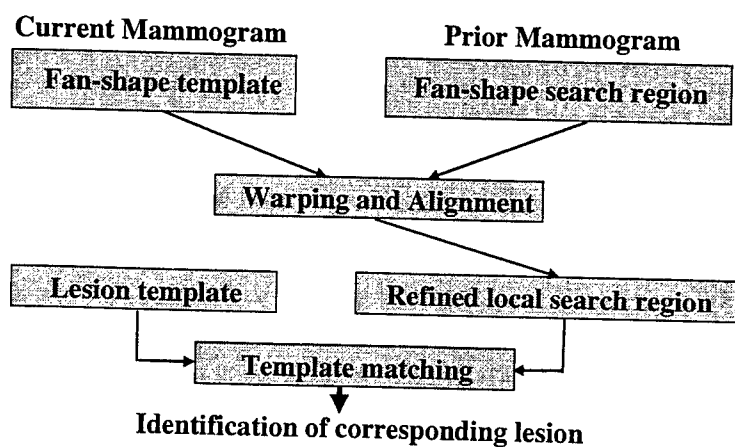


Figure 1. Block-diagram of the regional registration technique.

In the local alignment stage, the location of the search region on the prior mammograms was first refined by maximizing correlation measure between a template extracted from the current mammogram and the breast structures on the prior mammogram. The affine transformation in combination with simplex optimization was then employed to warp this local region. In the final stage a search for the best match between the lesion template from the current mammogram and a structure on the prior mammogram was carried out within the refined search region. A more detailed explanation for each of the stage will be presented in the following subsections.

### 2.1. Stage1: Global alignment

Initially an automatic procedure is used to detect the breast boundary for all of the mammograms (Fig. 2). In the first stage the breast images from the current and prior mammograms were globally aligned by maximizing a mutual information measure. The nipple locations of the two breast images were used as the pivot points in a common reference frame for the alignment.

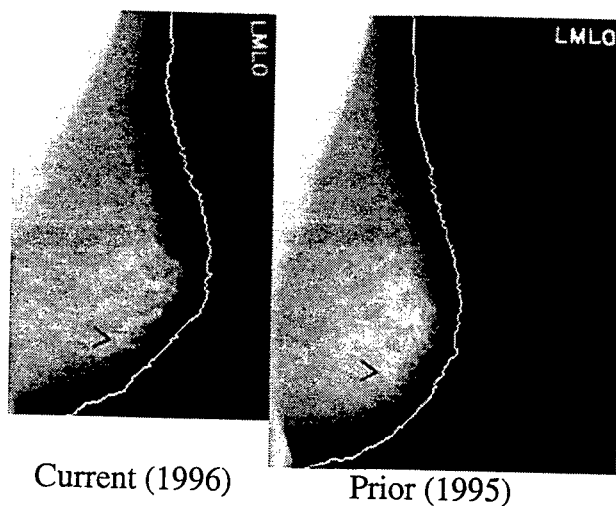


Figure 2. Current and prior mammogram. The arrows point to the masses on the current and the prior mammograms.

### 2.2. Stage 1: Definition of fan-shape regions

The location of the mass on the current mammogram is determined in a polar coordinate system with the nipple as the origin. The location is represented as the radial distance from the nipple and the angle between the nipple-mass centroid axis and the breast periphery. Angular and radial scaling are performed and the position of the mass on the prior mammogram is predicted in a polar coordinate system defined in a similar manner (Fig. 3). An initial fan-shape search region is then defined on the prior mammogram centered at the predicted location of the mass centroid (Fig. 4).

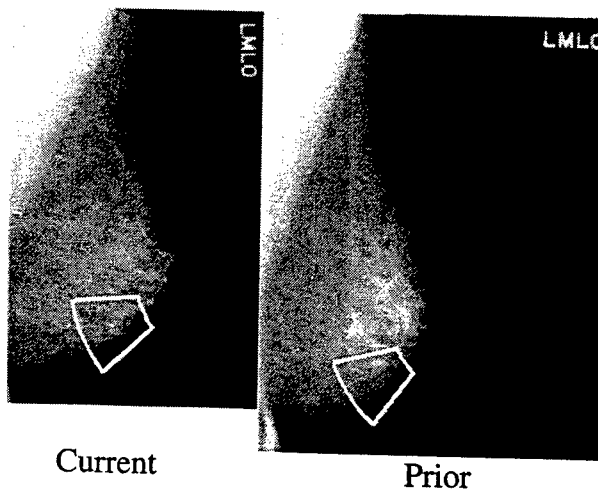
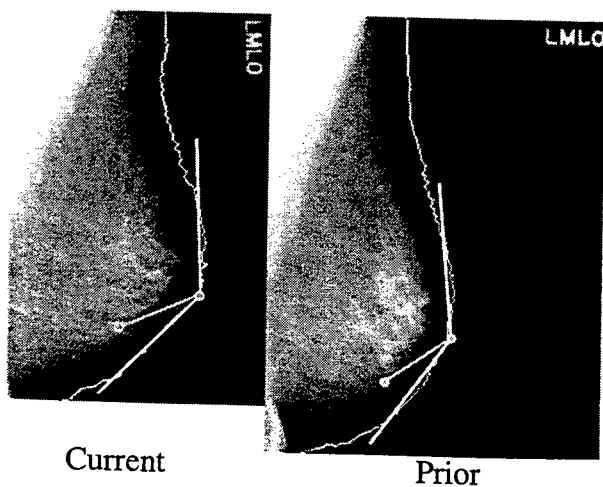


Figure 3. Initial estimation of the mass centroid position on the prior mammogram based on the nipple-mass distance and the angle between the nipple-mass axis and breast periphery on the current mammogram.

Figure 4. Definition of an initial fan-shape search region on the prior mammogram and a fan-shape template on the current mammogram.

The size of the fan-shape region is predefined using a training set so that it will include the mass centroid on the prior mammograms. A fan-shape template centered at the mass is also defined on the current mammogram.

### 2.3. Stage 2: Warping and alignment

In the second stage the fan-shape search region is refined. By allowing warping of the fan-shape template from the current mammogram, it may provide better compensation for local geometric distortions due to differences in positioning of the breast and in breast compression and may improve the localization of the mass on the prior mammogram. The warping procedure is based on the affine transformation combined with simplex optimization. In the following the warping procedure is explained in greater detail.

#### 2.3.1. Affine transformation

An affine transformation<sup>13</sup> is a linear transformation combining rotation and translation. A two dimensional affine transformation is defined as follows:

$$\begin{aligned}x' &= ax + by + c \\y' &= dx + ey + f\end{aligned}\quad (1)$$

where  $(x, y)$  are the original coordinates,  $(x', y')$  are the transformed coordinates, and  $a, b, d, e, c, f$  are the transformation coefficients. The coefficients  $a, b, d, e$  determine a scaling and a rotation, and the coefficients  $c$  and  $f$  determine a translation. The result of the application of the affine transformation of Eq. (1) in combination with simplex optimization (described below) is shown in Fig. 5. Since the affine transformation is linear, the transformed objects are linearly resized and rotated. This can be observed from the edges of the fan-shape region bounding box (the white box in Fig. 5). After the transformation the edges are still straight lines, however, the corner angles are different from 90 degrees and the length of the lines is also linearly scaled.

#### 2.3.2. Nonlinear Simplex Optimization

The Nelder and Mead<sup>14,15</sup> nonlinear simplex optimization is used in order to adjust the coefficients  $a, b, c, d, e$  and  $f$  and to warp the fan-shaped template in order to maximize the correlation between the template and a breast structure on the prior mammogram. This optimization defines a hyper polygon. For each vertex an error function is calculated. Then the polygon is "rolled" towards the minimum. The movement of the polygon (toward the minimum) is obtained by the reflection in the direction opposite to the vertex with maximal error. Fig. 5 shows the result of application of the affine transformation whose coefficients were obtained by the nonlinear simplex optimization.

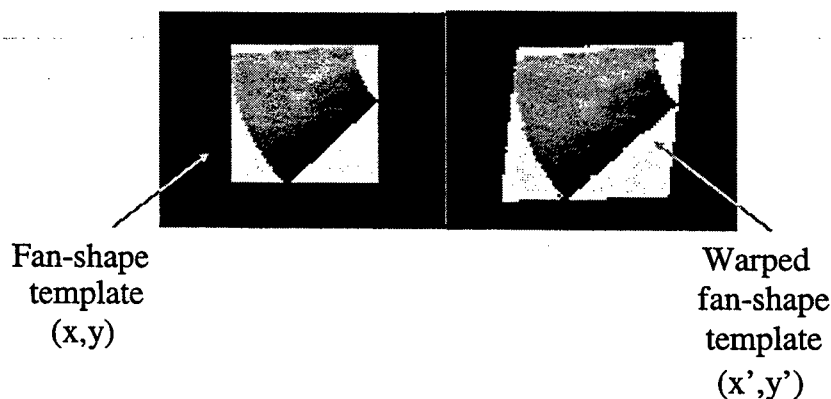


Figure 5. Fan-shaped template and warped fan-shaped template by the affine transformation.

#### 2.4. Mass template alignment and identification of corresponding lesion

In this stage a new search region with a reduced size is defined on the prior mammogram (Fig. 6). A template containing the mass is extracted from the current mammogram. Then, the mass location on the prior mammogram is determined by maximizing the correlation between the template and a structure within the search region (Fig. 7).

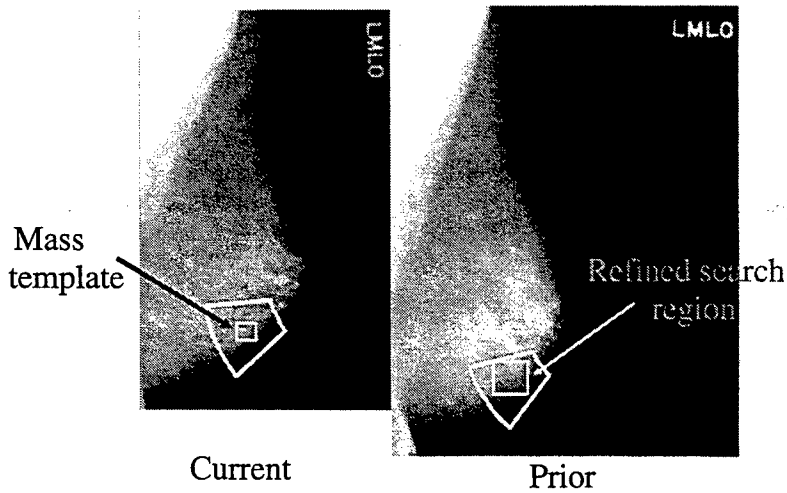


Figure 6. A refined search region is defined on the prior mammogram. A search for the best match between the mass template from the current mammogram and a structure on the prior mammogram was carried out within the refined search region.

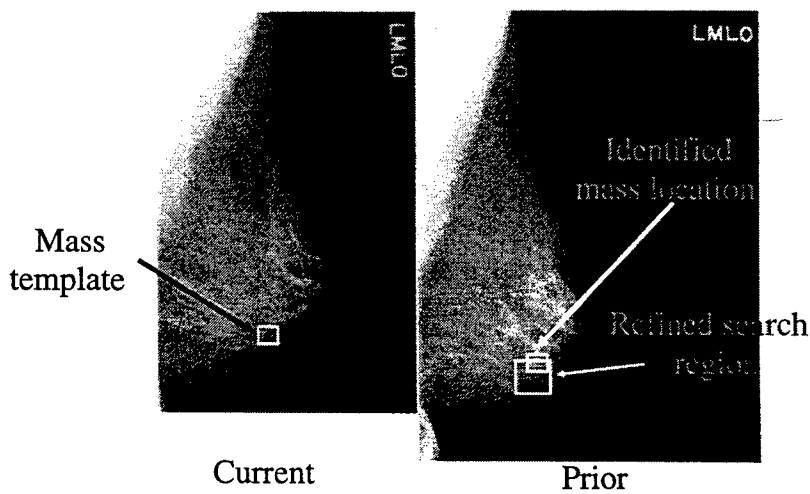


Figure 7. Final identification of the corresponding mass on the prior mammogram.

### 3. DATA SET

A set of 124 temporal pairs of mammograms containing biopsy-proven masses on the current mammograms was used to examine the performance of this approach. A total of 221 mammograms from 43 cases were digitized. Thirty five of the mammograms were digitized with a LUMISYS DIS-1000 laser scanner at a pixel resolution of  $100 \mu\text{m} \times 100 \mu\text{m}$  and 4096 gray levels. The digitizer was calibrated so that gray level values were linearly proportional to the optical density (OD) within the range of 0.1 to 2.8 OD units, with a slope of 0.001 OD/pixel value. Outside this range, the slope of the calibration curve decreased gradually. The OD range of the digitizer was 0 to 3.5. The remaining 186 mammograms were digitized with a LUMISCAN 85 laser scanner at a pixel resolution of  $50 \mu\text{m} \times 50 \mu\text{m}$  and 4096 gray levels. The digitizer was calibrated so that gray level values were linearly proportional to the OD within the range of 0 to 4 OD units, with a slope of 0.001 OD/pixel value. Output from both digitizers was linearly converted so that a large pixel value corresponded to a low optical density. In order to process the mammograms digitized with these two different digitizers, the images digitized with LUMISCAN 85 digitizer were averaged with a  $16 \times 16$  box filter, resulting in  $800 \mu\text{m}$  images. The images digitized with LUMISYS DIS-1000 digitizer were averaged with a  $8 \times 8$  box filter, resulting in  $800 \mu\text{m}$  images. The true lesion locations were identified by an experienced radiologist on all mammograms. The 221 mammograms contained 219 biopsy-proven and 2 follow-up masses. From all 124 temporal pairs of mammograms, 63 were CC-view pairs, 48 were MLO-view pairs, and 13 were lateral-view pairs.

### 4. EVALUATION METHODS

The accuracy of the multistage regional registration was analyzed in terms of two measures. The first measure is the overlap area between the estimated and the true lesions on the prior mammogram. The fractions of registered temporal pairs that could provide an accuracy of over 50% area overlap and over 75% area overlap were examined. The second measure is the average Euclidean distance between the centroids of the estimated and true lesion locations.

### 5. REGISTRATION RESULTS

In this study 86% of the estimated lesion locations resulted in an area overlap of at least 50% with the true lesion locations. The average distance between the estimated and the true centroids of the lesions on the prior mammogram was  $4.4 \pm 5.9$  mm with a maximum of 30.6 mm. These results are presented in Table 1 and Table 2. For the 86% of the temporal pairs with 50% overlap, the average distance between the estimated and the true centroids of the lesions on the prior mammogram was  $2.4 \pm 2.1$  mm with a maximum of 10.2 mm.

Table 1. The area overlap between the true and the estimated masses on the prior mammogram.

Pairs	50% overlap	75% overlap
Number	107	99
%	86%	80%

Table 2. The distance between the true and the estimated centroids of the mass on the prior mammogram.

	Overall	50% overlap	75% overlap
Mean distance	4.4 mm	2.4 mm	2.2 mm
Standard. Deviation.	5.9 mm	2.1 mm	2.0 mm
Max. distance	30.6 mm	10.2 mm	10.2 mm

### 6. CONCLUSION

The regional registration technique can localize the corresponding mass on the prior mammogram. The warping procedure based on an affine transformation in the local alignment stage reduces the size of the search region. Eighty-six percent of the

estimated lesion locations resulted in an area overlap of at least 50% with the true lesion locations. The average distance between the estimated and the true centroids of the lesions on the prior mammogram was  $4.4 \pm 5.9$  mm. When the threshold was set to 75% area overlap, 80% of the temporal pairs could still exceed the threshold. The registration accuracy of the current method has been improved in comparison with that of our previous method,<sup>10</sup> although the data set was increased from 74 pairs to 124 pairs. This improvement is obtained mainly from the second stage affine transformation and simplex optimization. Further study is underway to develop a feature matching method to improve lesion localization within the search region.

### ACKNOWLEDGMENTS

This work is supported by a Career Development Award from the USAMRMC (DAMD 17-98-1-8211) (L.H.), a USPHS Grant CA 48129, a USAMRMC grant (DAMD 17-96-1-6254).

### REFERENCES

1. H. C. Zuckerman, "The role of mammography in the diagnosis of breast cancer," in *Breast Cancer, Diagnosis and Treatment*, edited by I. M. Ariel and J. B. Cleary (McGraw-Hill, New York, 1987), pp. 152-172.
2. L. Tabar and P. B. Dean, "The control of breast cancer through mammographic screening: What is the evidence," *Radiol. Clin. N. Amer.* **25**, pp. 993-1005, 1987.
3. L. W. Bassett, B. Shayestehfar and I. Hirbawi, "Obtaining previous mammograms for comparison: usefulness and costs," *Amer. J. Roentgenology* **163**, pp. 1083-1086, 1994.
4. E. A. Sickles, "Periodic mammographic follow-up of probably benign lesions: results in 3183 consecutive cases," *Radiology* **179**, pp. 463-468, 1991.
5. M. Sallam and K. Bowyer, "Detecting abnormal densities in mammograms by comparison with previous screenings" in *Digital Mammography '96*, edited K. Doi, M. L. Giger, R. M. Nishikawa and R. A. Schmidt (Elsevier, Amsterdam, 1996).
6. D. Brzakovic, N. Vujovic, M. Neskovic, P. Brzakovic and K. Fogarty, "Mammogram analysis by comparison with previous screenings" in *Digital Mammography '96*, edited by K. Doi, M. L. Giger, R. M. Nishikawa and R. A. Schmidt (Elsevier, Amsterdam, 1996).
7. N. Vujovic and D. Brzakovic, "Establishing the correspondence between control points in pairs of mammographic images," *IEEE Trans. Imag. Proc.* **6**, pp. 1388-1399, 1997.
8. S. Sanjay-Gopal, H. P. Chan, B. Sahiner, N. Petrick, T. Wilson, M. Helvie, "Evaluation of interval change in mammographic features for computerized classification of malignant and benign masses," *Radiology* **205(P)**, pp. 216, 1997.
9. S. Sanjay-Gopal, H. P. Chan, N. Petrick, T. Wilson, B. Sahiner, M. Helvie, M. Goodsitt, "A regional registration technique for automated analysis of interval changes of breast lesions," *Proc. SPIE* **3338**, pp. 118-131, 1998.
10. S. Sanjay-Gopal, H.P. Chan, T.E. Wilson, M.A. Helvie, N. Petrick, B. Sahiner, "A regional registration technique for automated interval change analysis of breast lesions on mammograms", *Medical Physics*, **26**: pp. 2669-2679, 1999.
11. L. Hadjiiski, H.P. Chan, B. Sahiner, N. Petrick, M.A. Helvie, S.S. Gopal, "Automated identification of breast lesions in temporal pairs of mammograms for interval change analysis", *Radiology*, **213(P)**: pp. 229-230, 1999.
12. W. Good, B. Zheng, Y.H. Chang, X. Wang, G. Maitz, "Generalized procrustean image deformation for subtraction of mammograms", *Proc. SPIE* **3661**, pp. 1562-1573, 1999.
13. L. Quan, T. Kanade, "Affine structure from line correspondance with uncalibrated affine cameras", *IEEE Trans. Pat. Anal. Machine Intel.*, Vol. 19, No. 8, Aug. 1997.
14. S.S. Rao, *Optimization: Theory and Applications*, Wiley Eastern Limited, 1979.
15. F.A. Lootsma, (ed). *Numerical methods for non-linear optimization*, Academic Press, New York, 1972.